Reconstructing the neutron-star equation of state from astrophysical measurements

Feryal Özel and Dimitrios Psaltis

Department of Astronomy and Steward Observatory, University of Arizona, 933 N. Cherry Avenue, Tucson, Arizona 85721, USA
(Received 4 May 2009; revised manuscript received 11 August 2009; published 5 November 2009)

The properties of matter at ultrahigh densities, low temperatures, and with a significant asymmetry between protons and neutrons can be studied exclusively through astrophysical observations of neutron stars. We show that measurements of the masses and radii of neutron stars can lead to tight constraints on the pressure of matter at three fiducial densities, from 1.85 to 7.4 times the density of nuclear saturation, in a manner that is largely model independent and that captures the key characteristics of the equation of state. We demonstrate that observations with 10% uncertainties of at least three neutron stars can lead to measurements of the pressure at these fiducial densities with an accuracy of 0.11 dex or $\simeq 30\%$. Observations of three neutron stars with 5% uncertainties are sufficient to distinguish at a better than 3σ confidence level between currently proposed equations of state. In the electromagnetic spectrum, such accurate measurements will become possible for weakly magnetic neutron stars during thermonuclear flashes and in quiescence with future missions such as the International X-ray Observatory.

I. INTRODUCTION

Matter in the deep interiors of neutron stars is characterized by low temperatures, large chemical potentials, and a significant asymmetry between the number of neutron and protons. In these conditions, several phenomena may take place, such as the creation of stable bosons and hyperons or a phase transition to quark matter. In addition, at these high densities, the symmetry energy of nucleonic matter plays a dominant role in determining its microscopic properties. The large uncertainty in understanding these phenomena has led to a wide range of models for the equation of state of neutron-star matter, which cannot be distinguished by hadron collision experiments or with observations of the early universe [1,2].

The relation between the pressure P and density ρ of neutron-star matter determines the macroscopic properties of the stars and, in particular, their radii R, masses M, and moments of inertia I. In fact, there is a unique map between the microscopic $P - \rho$ relation and the macroscopic $M - R$ one [3]. Astrophysical observations of neutron stars aim to exploit this mapping and invert it in order to measure their equation of state.

The mass and radius of a neutron star of a given central density, ρ_c, depend on the entire relation between pressure and density up to ρ_c, because of the density gradient from the center of the star to its surface. If the mass-radius relation could be traced observationally with a large number of neutron stars spanning the entire range of masses (e.g., 0.2–$2M_\odot$), then the mapping could be formally inverted to generate the complete equation of state [3]. However, the astrophysical formation channels for neutron stars limit them to masses larger than $\simeq 1.2M_\odot$, rendering this approach impractical.

Lattimer and Prakash [2] studied extensively the properties of neutron-star models for a large range of equations of state and concluded that the predicted radii depend primarily on the pressure at a fiducial density, comparable to the nuclear saturation density of $\rho_{ns} \sim 2.7 \times 10^{14}$ g cm^{-3}. More recently, Read *et al.* [4] showed that not only the approximate radii of neutron stars, but a large number of observables depend on a small number of parameters that characterize the equation of state.

In this paper, we show that the masses and radii of neutron stars act as tracers of the pressure of neutron-star matter at three fiducial densities. In other words, the complete mass-radius relation to high accuracy can be reproduced for all proposed equations of state, when the pressure at these three densities is specified. Therefore, a one-to-one mapping exists between the pressure at the three densities and the mass-radius relation, which can be inverted even if the observed neutron stars are confined to a small range of masses. We present the formalism for this inversion that takes into account the uncertainties in the mass and radius measurements and show that observations of three neutron stars with a 10% uncertainty can lead to a measurement of the pressure of ultradense matter at these densities with comparable accuracy.

II. A MINIMAL REPRESENTATION OF NEUTRON-STAR EQUATIONS OF STATE

Inferring the pressure of neutron-star matter at a large number of densities from astrophysical measurements would ideally generate the equation of state in a model-independent way. However, the range of core densities of neutron stars with masses $\gtrsim 1.2M_\odot$ is in fact not very large and, therefore, the pressure at a small number of fiducial densities ρ_i governs their observable properties. Choosing two fiducial densities, setting them to the fixed values $\rho_1 = 1.85\rho_{ns}$ and $\rho_2 = 2\rho_1$, and assuming a piecewise polytropic relation between them has been shown to accurately

103003-1

reproduce the complete pressure-density relation for a large sample of proposed equations of state [4].

We explored the predicted mass-radius relations for the parametric equation of state of Ref. [4] in which the polytropic indices between the fiducial densities are left as free parameters. We found that different combinations of polytropic indices lead to practically indistinguishable mass-radius relations for the neutron-star models. Consequently, this choice leads to a significant degeneracy between the inferred uncertainties of the various model parameters when aiming to reconstruct the equation of state from a set of mass-radius measurements (see Sec. III). This degeneracy is greatly reduced if we choose, instead, the values of $P(\rho_1)$ and $P(\rho_2)$ to be the free parameters and describe the equation of state at densities larger than ρ_2 by a polytrope with normalization set by the pressure $P(\rho_3)$ at a third fiducial density $\rho_3 > \rho_2$. Because the density ρ_3 only serves to specify the polytropic index at densities larger than ρ_2, its exact value does not affect the final result. Hereafter, we set $\rho_3 = 2 \times \rho_2$. Following Ref. [4], we supplement this with the equation of state SLy [5] for the outer layers of the neutron star for densities below a ρ_0, which we leave as a free parameter.

Specifically, we use hereafter the following parametric equation of state of neutron-star matter, which depends on four parameters ρ_0, $P_1 \equiv P(\rho_1)$, $P_2 \equiv P(\rho_2)$, and $P_3 \equiv P(\rho_3)$.

(i) For $\rho \leq \rho_0$, we interpolate between the tabulated values of the SLy equation of state [5]. We define P_0 and ϵ_0 to be the pressure and energy density at ρ_0, respectively.

(ii) For $\rho_0 < \rho \leq \rho_1$, we define

$$\Gamma_1 \equiv \frac{\log(P_1/P_0)}{\log(\rho_1/\rho_0)}, \tag{1}$$

so that the pressure in this density range is given by

$$P = P_1 \left(\frac{\rho}{\rho_1}\right)^{\Gamma_1}, \tag{2}$$

and the energy density is

$$\epsilon = (1 + a_1)\rho + \frac{P_1}{\Gamma_1 - 1}\left(\frac{\rho}{\rho_1}\right)^{\Gamma_1}, \tag{3}$$

where

$$a_1 = \frac{\epsilon_0}{\rho_0} - 1 - \frac{P_1}{(\Gamma_1 - 1)\rho_0}\left(\frac{\rho_0}{\rho_1}\right)^{\Gamma_1}. \tag{4}$$

(iii) For $\rho_1 < \rho \leq \rho_2$, we set

$$\Gamma_2 \equiv \frac{\log(P_2/P_1)}{\log(\rho_2/\rho_1)}, \tag{5}$$

so that the pressure in this density range is given by

$$P = P_1 \left(\frac{\rho}{\rho_1}\right)^{\Gamma_2}, \tag{6}$$

and the energy density is

$$\epsilon = (1 + a_2)\rho + \frac{P_1}{\Gamma_2 - 1}\left(\frac{\rho}{\rho_1}\right)^{\Gamma_2}, \tag{7}$$

where

$$a_2 = a_1 + \frac{P_1}{(\Gamma_1 - 1)\rho_1} - \frac{P_1}{(\Gamma_2 - 1)\rho_1}. \tag{8}$$

(iv) For $\rho > \rho_2$, we set

$$\Gamma_3 \equiv \frac{\log(P_3/P_2)}{\log(\rho_3/\rho_2)}, \tag{9}$$

so that the pressure in this density range is given by

$$P = P_2 \left(\frac{\rho}{\rho_2}\right)^{\Gamma_3}, \tag{10}$$

and the energy density is

$$\epsilon = (1 + a_3)\rho + \frac{P_2}{\Gamma_3 - 1}\left(\frac{\rho}{\rho_2}\right)^{\Gamma_3}, \tag{11}$$

where

$$a_3 = a_2 + \frac{P_1}{(\Gamma_2 - 1)\rho_2}\left(\frac{\rho_2}{\rho_1}\right)^{\Gamma_2} - \frac{P_2}{(\Gamma_3 - 1)\rho_2}. \tag{12}$$

Figure 1 shows the mass-radius relations obtained by integrating the Tolman-Oppenheimer-Volkoff equations with the complete (solid lines) as well as the parametric (dashed lines) forms of a sample of proposed equations of state, chosen to represent a wide range of physical conditions (see Table I for the parameters). The three examples also span a large range in neutron-star masses and radii. For neutron stars with masses $>1M_\odot$, the deviation in radius between the models with the complete and parametric equations of state is always $\leq 2\%$. The same is true for all the equations of state considered in Ref. [4].
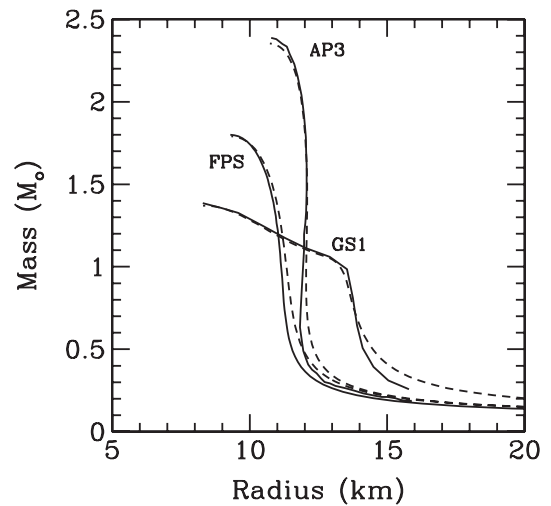

FIG. 1. Mass-radius relations for neutron stars, computed using the complete (solid lines) as well as the parametric (dashed lines) forms of three equations of state.

TABLE I.   Best-fit equation-of-state (EOS) parameters for three sample equations of state.

EOS	$\log\rho_0$	$\log P_1$	$\log P_2$	$\log P_3$
FPS	14.30	34.283	35.142	35.925
GS1	14.85	34.504	34.884	35.613
AP3	14.30	34.392	35.464	36.452

In order to get an intuitive understanding of the effect of these parameters, we show in Fig. 2 how the calculated mass-radius relations change when we vary each parameter in succession away from the best-fit values for equation of state FPS. (For the names and details of the equations of state, see Ref. [2].) The value of the pressure at ρ_1 determines predominantly the characteristic radii of neutron stars; this is the effect described in Ref. [2]. The value of the pressure at ρ_2 regulates the slope of the mass-radius relation, at larger masses. The pressure at ρ_3 sets the maximum mass of neutron stars. Finally, the value of the density ρ_0, where the parametric branch of the equation of state begins, only affects the mass-radius relation at small neutron-star masses. In the first three cases, the parameters are varied by 25% away from their best-fit value in each direction while, in the last case, the density ρ_0 is reduced to 1/2 and 1/4 of its original value in order to give rise to a
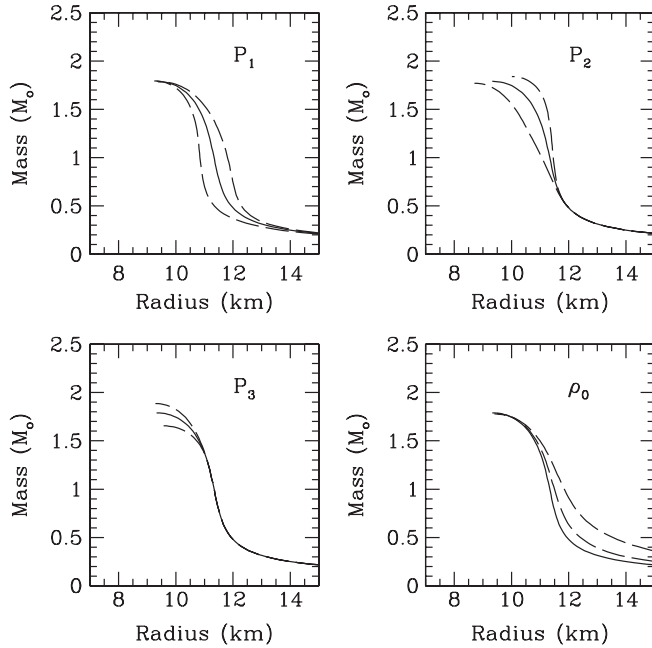

FIG. 2.   The dependence of the calculated mass-radius relations of neutron stars on the parametric equation of state. The first three panels show the change in the predicted relation when the values of the parameters P_1, P_2, and P_3 are varied by 25% in each direction away from the best-fit values for the equation of state FPS. The last panel shows the change in he predicted relation when the value of the parameter ρ_0 is reduced to 1/2 and 1/4 of its best-fit value for the same equation of state.

visible difference in the resulting mass-radius relation. Because of the much weaker dependence of the observed properties of neutron stars on ρ_0, especially at the mass range $\gtrsim 1.2M_\odot$ of interest, we fix hereafter its value to $\log\rho_0 = 14.30$.

The distinct dependences of the mass-radius relations on the values of the three parameters P_1, P_2, and P_3 shown in Fig. 2 will allow a determination of each parameter from observations with minimal correlated uncertainties. Moreover, the rather strong dependence of the mass-radius relations on the parameters of the equation of state guarantees that these parameters can be accurately measured from astrophysical observations. We discuss the expected uncertainties in the following section.

III. EQUATION-OF-STATE PARAMETER ESTIMATION FROM MEASUREMENTS OF MASSES AND RADII

The mass-radius relation of neutron stars that can be probed by astrophysical observations is determined to a large extent by the three parameters P_1, P_2, and P_3 of the parametric equation of state that we discussed in the previous section. This is because the value of the fourth parameter, ρ_0, only affects significantly the properties of neutron stars with masses that are too low to be astrophysically relevant.

For a given equation of state, the particular realization of a neutron star is determined by its central density ρ_c. As a result, independent mass and radius measurements of N neutron stars require $N + 3$ parameters to be completely modeled, under the assumption that all stars follow the same equation of state. In other words, observations of N neutron stars yield $2N$ measurements, while modeling their properties requires $N + 3$ parameters, leaving $2N - (N + 3) = N - 3$ degrees of freedom. Thus, in order to obtain a unique solution, at least three neutron-star mass and radius measurements are required. Hereafter, we discuss the situation with $N = 3$.

Our aim is to invert the one-to-one map between the parameter space of the observables $(R_1, M_1, R_2, M_2, R_3, M_3)$ to the one of the physical quantities $(P_1, P_2, P_3, \rho_{c,1}, \rho_{c,2}, \rho_{c,3})$, where the indices on the masses, radii, and central densities refer to the three observed neutron stars. Because of the uncertainties inherent to the measurements, we actually need to convert a probability distribution density over the parameter space of observables $\mathcal{P}_{obs}(R_1, M_1, R_2, M_2, R_3, M_3)$ to one over the physical parameters $\mathcal{P}(P_1, P_2, P_3, \rho_{c,1}, \rho_{c,2}, \rho_{c,3})$. The particular values of the central densities for the three stars are not of particular interest and obtaining the final probability density over the equation-of-state parameters P_1, P_2, and P_3 would require marginalizing over the three central densities. In order to avoid this additional complication, we choose instead to transform the probability density from the parameter space of observables to one over

$(P_1, P_2, P_3, M_1, M_2, M_3)$ and then marginalize over the three neutron-star masses. Formally, we write

$$
\begin{aligned}
&\mathcal{P}(P_1, P_2, P_3, M_1, M_2, M_3) \\
&\quad = \mathcal{P}_{\mathrm{obs}}(R_1, M_1, R_2, M_2, R_3, M_3)\mathcal{J}\!\left(\frac{R_1, R_2, R_3}{P_1, P_2, P_3}\right),
\end{aligned}
\tag{13}
$$

where the last term is the Jacobian of the transformation between the three observed radii and the three parameters of the equation of state.

For each set of parameters of the equation of state P_1, P_2, P_3, we obtain the relation between neutron-star radius and mass, $R = R(M; P_1, P_2, P_3)$, by integrating the Tolman-Oppenheimer-Volkoff equation and use it to calculate numerically the Jacobian as

$$
\mathcal{J}\!\left(\frac{R_1, R_2, R_3}{P_1, P_2, P_3}\right) \equiv \det(\mathcal{J}_{ij}) = \det\!\left(\frac{\partial R}{\partial P_i}\bigg|_{M_j}\right).
\tag{14}
$$

We then integrate Eq. (13) over the three neutron-star masses to obtain the final probability distribution over the parameters of the equation of state

$$
\begin{aligned}
\mathcal{P}(P_1, P_2, P_3) = &\iiint dM_1 dM_2 dM_3 \\
&\times \mathcal{P}(P_1, P_2, P_3, M_1, M_2, M_3).
\end{aligned}
\tag{15}
$$

In order to study the accuracy with which the equation-of-state parameters can be inferred from astrophysical measurements and to assess the potential correlations between them, we simulated mass-radius data for three neutron stars that obey the FPS equation of state, chosen here as an example. In particular, we set $M_1 = 1.50 M_\odot$, $R_1 = 10.7$ km, $M_2 = 1.61 M_\odot$, $R_2 = 10.5$ km, $M_3 = 1.70 M_\odot$, $R_1 = 10.2$ km, and assigned to each measurement an in-

dependent Gaussian uncertainty with standard deviation equal to 5% and 10% of the corresponding central values. We show the simulated data in Fig. 3 together with their uncertainties. Note that this is a very conservative and narrow range of measurements for neutron-star masses, as observed masses have been reported ranging from $\simeq 1.2 M_\odot$ in radio pulsars [6] to $\simeq 2.1 M_\odot$ in accreting neutron stars [7]. We will discuss at the end of this section the improved constraints on the equation of state that can be obtained when a wider range of masses is considered.

Using this set of simulated measurements, we inverted the mapping between neutron-star mass radius and the equation-of-state pressures at three fiducial densities and calculated the probability distribution over the three parameters P_1, P_2, and P_3 according to Eqs. (13)–(15). Because the resulting probability density is defined in a three-dimensional parameter space, we show, in the following set of figures, projections and marginalizations of this function along different directions.

In Fig. 4, we show the normalized probability density over the pressure P_2 at the fiducial density ρ_2, evaluated when the other two parameters of the equation of state are set to the best-fit values for equation of state FPS (see Table I). The true value of the pressure P_2 for equation of state FPS, shown by the vertical dashed line, is within 0.02 dex or 4.7% of the peak of the probability distribution. Moreover, the parameter P_2 is tightly constrained with a 1σ uncertainty of 0.11 dex or 29%.
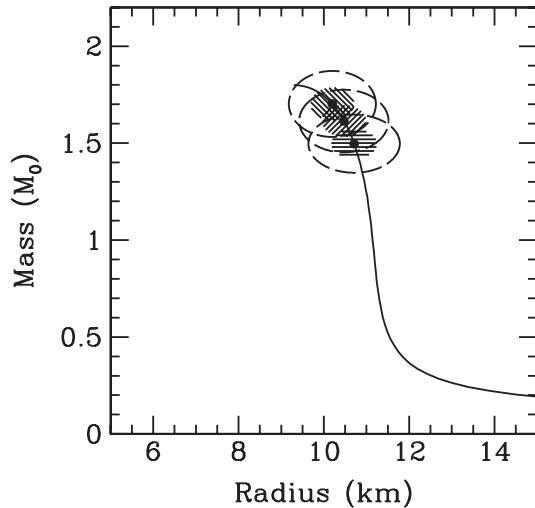

FIG. 3. Simulated values of the masses and radii of three neutron stars that obey the FPS equation of state (solid dots). The hatch-filled regions and the ellipses indicate 5% and 10% uncertainties in each measurement, respectively.
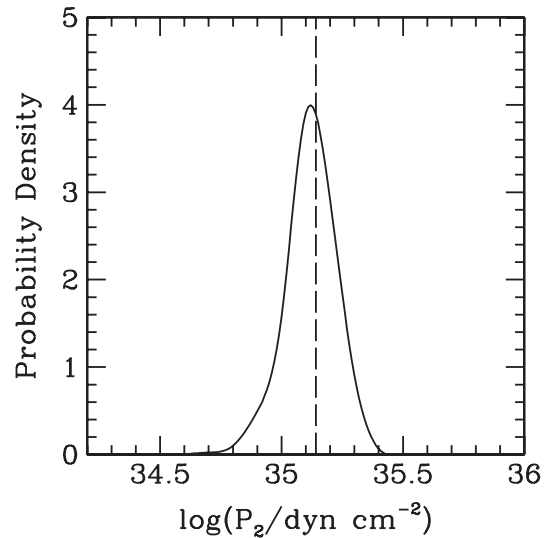

FIG. 4. The probability density over the pressure P_2 at 3.7 times the nuclear saturation density, evaluated when the other two parameters of the equation of state are set to the best-fit values for equation of state FPS. This is the probability that the parametric equation of state reproduces the set of simulated data shown in Fig. 3 that have 10% measurement uncertainties. The vertical dashed line indicates the true pressure at density ρ_2 of the FPS equation of state.
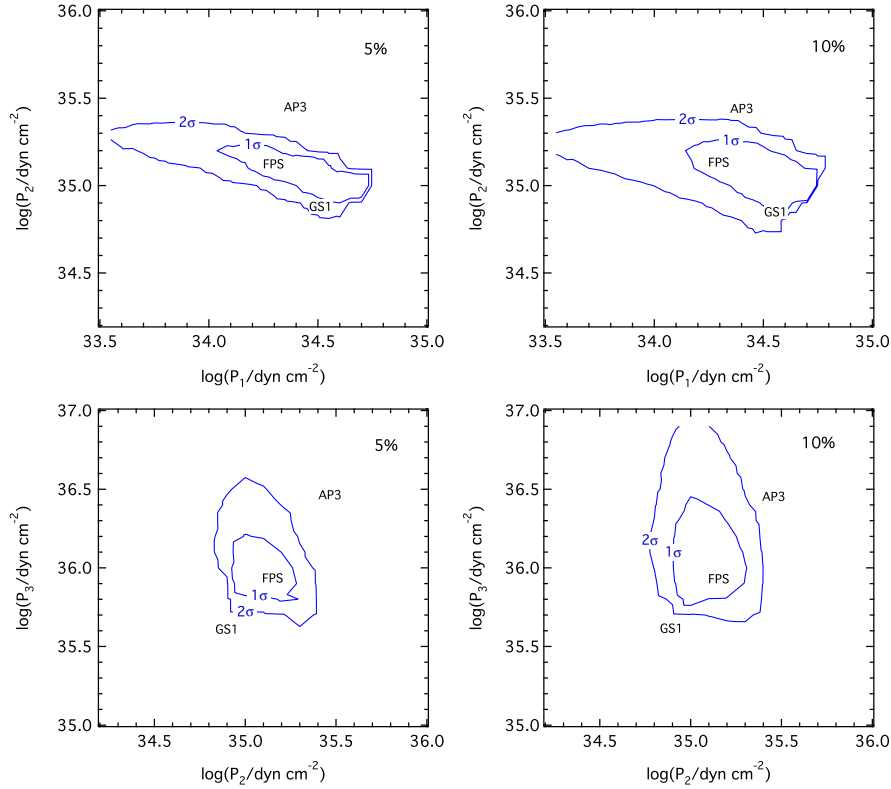
FIG. 5 (color online).   Contours of 68.2% (1σ) and 95.4% (2σ) confidence levels for the values of pairs of parameters of the equation of state necessary to describe the simulated data shown in Fig. 3. In each panel, the probability density is marginalized over the parameter not shown. The parameters P_1, P_2, and P_3 are the pressures at 1.85, 3.70, and 7.40 times the nuclear saturation density, respectively. In all panels, the corresponding true pressures for a sample of proposed equations of state are shown for comparison. The left panels correspond to a 5% uncertainty in the measurements, whereas the right panels correspond to a 10% uncertainty. A 5% measurement error is sufficient to distinguish to a better than 3σ level not only between equations of state that have different underlying physics but also between ones with similar mass-radius predictions.

In Fig. 5, we show the normalized two-dimensional probability distributions over different pairs of the equation-of-state parameters, marginalized over the remaining parameter. In each panel, the two contours correspond to the 68.2% (1σ) and 95.4% (2σ) confidence levels. In all panels, the true pressures for a set of representative equations of state are shown for comparison. Finally, the left and right panels show the probability densities obtained for the assumed 5% and 10% uncertainties in the simulated data, respectively.

The results shown in the same figure provide additional justification for the use of three (as opposed to fewer) fiducial densities at which to measure the pressure of matter. In Ref. [4], which showed that many proposed equations of state can be described by a piecewise polytropic model, this was necessitated by that fact that the potential production of bosons or hyperons at high densities or a phase transition to quark matter causes abrupt changes to the equation of state at multiple densities. Here, the use of three fiducial densities allows us to distinguish between equations of state, without requiring unattainable accuracy in the measurements. In the examples shown in

Fig. 5, while both equations of state FPS and GS1 are consistent with the simulated data in the $P_1 - P_2$ parameter space, equation of state GS1 can be excluded at a confidence better than $2 - 3\sigma$ in the $P_2 - P_3$ space.
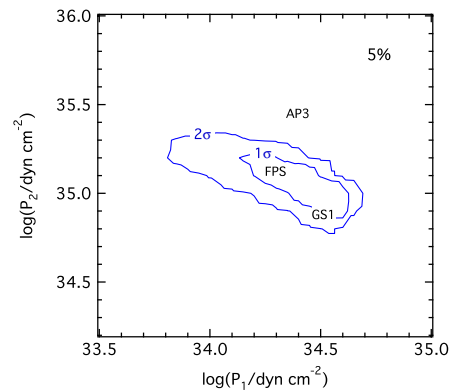

FIG. 6 (color online).   The tightening of the constraints on the equation-of-state parameter P_1 compared to the upper-left panel in Fig. 5, when a $1.3M_\odot$ neutron star is included in the simulated data.
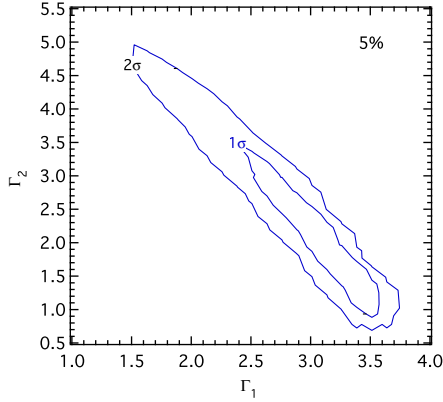
FIG. 7 (color online). The constraints on the polytropic indices Γ_1 and Γ_2, which appear in the alternative parametrization of the equation of state, obtained for the same simulated data as in Fig. 6. This parametrization leads to significantly correlated uncertainties even for the wide range of neutron-star masses considered here and for 5% errors in the measurements.

Of the three pressures P_1, P_2, and P_3, the one at 3.7 times nuclear saturation density, i.e., P_2, is the most tightly constrained by the data. This is because of the particular range of masses that comprise our simulated data, for which the central density is comparable to ρ_2. The pressure P_1 at 1.85 times nuclear saturation density determines mostly the equation of state outside of the cores of these neutron stars and is, therefore, more tightly constrained from above (see the top panels of Fig. 5). On the other hand, the pressure P_3 at 7.4 times nuclear saturation density primarily affects the maximum allowed mass for neutron stars and is, therefore, more tightly constrained from below (see the bottom panels of Fig. 5).

The above discussion suggests that allowing for a wider range of masses in the simulated data would have improved the constraints on P_1, if the range extended to lower neutron-star masses, and on P_3, if the range included higher masses. We illustrate this for the case of P_1 in Fig. 6, where we have assumed that the three neutron stars have $M_1 = 1.31 M_\odot$, $R_1 = 10.95$ km, $M_2 = 1.50 M_\odot$, $R_2 = 10.7$ km, and $M_3 = 1.70 M_\odot$, $R_1 = 10.2$ km and allowed for 5% measurement uncertainties. Comparison with the top-left panel of Fig. 5 shows that the allowed range of values for the parameter P_1 has shrunk significantly when a lower-mass neutron star is included.

It is evident from Figs. 5 and 6 that the uncertainties in the three pressures P_1, P_2, and P_3 are weakly correlated. In fact, there is no discernible correlation between P_3 and the other two parameters. This motivated our choice of the three pressures as the parameters of the minimal representation of the equation of state as opposed to the polytropic indices between the corresponding densities (cf. [4]). Using the parametrization with polytropic indices would have resulted in correlated uncertainties, such as those shown in Fig. 7 for the case of Γ_1 and Γ_2, even for the

most constraining case of neutron-star masses and measurement errors considered above.

IV. DISCUSSION

In this paper, we have shown that measuring the masses and radii of three neutron stars with a 10% uncertainty can constrain to similar accuracy the pressure of neutron-star matter at densities several times the density of nuclear saturation. Moreover, astrophysical measurements with 5% uncertainties can distinguish, to a better than 3σ confidence level, not only between equations of state that have different underlying physics (e.g., FPS and GS1 in Fig. 5) but also between ones with very similar predicted mass-radius relations (e.g., FPS and AP3; see Fig. 1).

Several types of observations in the electromagnetic spectrum have already led to a number of mass and radius measurements for neutron stars in a wide variety of astrophysical systems. Dynamical measurements of the masses of radio pulsars in binary systems have uncertainties as low as 0.1% [6], but do not provide any information on the radii of the stars. As such, these observations can be used only to set lower bounds on the pressure at the three fiducial densities (and especially at ρ_2 and ρ_3) [4]. Similar constraints, albeit with much larger uncertainties, can also be set by the dynamical measurements of neutron-star masses in x-ray binaries, such as those reported for Vela X-1 [8] or Cyg X-2 [9]. At the same time, a secure identification as a black hole of a compact object that has a dynamically measured mass of $\simeq 2 M_\odot$ would place a stringent upper limit on the same parameters.

Measurements of both the masses and radii of neutron stars have been reported for weakly magnetic neutron stars in low-mass x-ray binary systems. In a number of cases, measurements were performed for globular cluster x-ray transients in quiescence, when the accretion practically ceases and the surface emission of the cooling neutron star can be directly observed [10,11]. These observations constrain the apparent radii of neutron stars and, therefore, lead to measurements of their masses and true radii with significant degeneracies. The degeneracies can be overcome, however, if the masses of the neutron stars are measured independently with dynamical observations of the binary systems in which they reside. Current observations with XMM-Newton led to $\simeq 15\%$ uncertainties in the measurements of the apparent radii [11]. Using a telescope with an effective area of 2 m^2, such as the one proposed for the International X-ray Observatory, would reduce this uncertainty to $\sim 5\%$.

A different set of measurements of both the masses and radii of weakly magnetic neutron stars were recently reported that utilized observations of their thermal emission during thermonuclear bursts [7,12]. The degeneracies between the inferred masses and radii were overcome in this case because up to three distinct observables that have different dependencies on the masses and radii were

used. In this case, the measurements were performed with the Rossi X-ray Timing Explorer and resulted in uncertainties of $\simeq 10\%$. Reducing the uncertainties to 5% requires an increase of the effective area of the telescope by a factor of $\simeq 4$, i.e., an effective area of 3.2 m^2. This is well within the design specifications of the Advanced X-ray Timing Array.

The masses and radii of neutron stars can in principle be constrained also by observing and modeling in detail the flux oscillations at the spin frequency of the neutron stars during the spreading of thermonuclear flashes [13]. This is not currently possible because it requires count rates significant larger than those achieved by the Rossi Explorer even for the brightest sources. Such measurements, however, may be achieved with future observations.

Dynamical measurements of the masses and moments of inertia of at least three neutron stars may also lead to very similar constraints as those discussed in this work [4,14]. Indeed, the moments of inertia of neutron stars of known masses encode not only information about their radii but of their density profiles, as well. As such, they are sensitive to the parameters of the equation of state at low densities and will lead to improved constraints on the parameters P_1 and ρ_0. For the case of the double pulsar, a measurement of the moment of inertia with an uncertainty of order 10% will probably be achieved by 2020 [15].

Finally, observations of the end stages of the coalescence of double neutron stars with gravitational wave observatories such as LIGO, VIRGO, and GEO-600 will open new avenues for measuring the masses and radii of neutron stars and, hence, for determining the properties of the equation of state of ultradense matter [16].

ACKNOWLEDGMENTS

[1] S. Hands, Contemp. Phys. **42**, 209 (2001).

[2] J. M. Lattimer and M. Prakash, Astrophys. J. **550**, 426 (2001).

[3] L. Lindblom, Astrophys. J. **398**, 569 (1992).

[4] J. S. Read, B. D. Lackey, B. J. Owen, and J. L. Friedman, Phys. Rev. D **79**, 124032 (2009).

[5] F. Douchin and P. Haensel, Astron. Astrophys. **380**, 151 (2001).

[6] S. E. Thorsett and D. Chakrabarty, Astrophys. J. **512**, 288 (1999).

[7] F. Özel, Nature (London) **441**, 1115 (2006).

[8] O. Barziv, L. Kaper, M. H. Van Kerkwijk, J. H. Telting, and J. Van Paradijs, Astron. Astrophys. **377**, 925 (2001).

[9] J. A. Orosz and E. Kuulkers, Mon. Not. R. Astron. Soc. **305**, 132 (1999).

[10] C. O. Heinke, G. B. Rybicki, R. Narayan, and J. E. Grindlay, Astrophys. J. **644**, 1090 (2006).

[11] N. A. Webb and D. Barret, Astrophys. J. **671**, 727 (2007).

[12] F. Özel, T. Güver, and D. Psaltis, Astrophys. J. **693**, 1775 (2009); T. Guver, F. Özel, A. Cabrera-Lavers, and P. Wroblewski, arXiv:0811.3979.

[13] T. E. Strohmayer, AIP Conf. Proc. **714**, 245 (2004).

[14] T. Damour and G. Schafer, Nuovo Cimento B **101**, 127 (1988); M. Bejger, T. Bulik, and P. Haensel, Mon. Not. R. Astron. Soc. **364**, 635 (2005); J. M. Lattimer and B. F. Schutz, Astrophys. J. **629**, 979 (2005); I. A. Morrison, T. W. Baumgarte, S. L. Shapiro, and V. R. Pandharipande, Astrophys. J. **617**, L135 (2004).

[15] M. Kramer and N. Wex, Classical Quantum Gravity **26**, 073001 (2009).

[16] J. S. Read, C. Markakis, M. Shibata, K. Uryu, J. D. E. Creighton, and J. L. Friedman, Phys. Rev. D **79**, 124033 (2009).